arXiv:1209.4466v1 [cond-mat.str-el] 20 Sep 2012

LDA+DMFT for organic molecular crystals: spectral and optical properties of κ-(BEDT-TTF)$_2$Cu[N(CN)$_2$]Cl

Johannes Ferber,* Kateryna Foyevtsova, Harald O. Jeschke, and Roser Valentí
Institut für Theoretische Physik, Goethe-Universität Frankfurt,
Max-von-Laue-Strasse 1, 60438 Frankfurt/Main, Germany

(Dated: September 21, 2012)

We present a combination of density functional theory with dynamical mean field theory to study correlation effects in organic layered charge-transfer salts. For that purpose, we propose a scheme to construct molecular Wannier functions using atomic orbitals as starting point. We compute spectral and optical properties of κ-(BEDT-TTF)$_2$Cu[N(CN)$_2$]Cl and demonstrate from first principles that interdimer transitions are strongly affected by correlations, leading to a Hubbard peak in the optical conductivity, while intradimer transitions are uncorrelated, giving rise to a peak consistent with LDA predictions. We discuss our results in the context of reported infrared reflection measurements.

PACS numbers: 71.27.+a,74.20.Pq,74.70.Kn,71.15.Ap,74.25.Gz,71.20.-b

Electron correlated materials show a rich phase diagram originating from the interplay of factors like magnetic ordering, frustration, doping, pressure, or temperature. Organic charge transfer (CT) salts are unique correlated systems with a complex phase diagram that can be finely tuned by chemical substitution or moderate pressures. Observed phases in these systems include metals, Fermi liquids, Mott insulators, antiferromagnets, spin liquids, and unconventional superconductors.[1,2]

An extensively studied class of CT salts are based on the molecules bis-(ethylenedithio)tetrathiafulvalene (BEDT-TTF, or shorter ET) crystallized in the κ phase. In these κ-(ET)$_2X$ salts, electron donors (ET) and electron acceptors (X) form alternating layers, with two ET molecules facing each other in ET dimers; these dimers are arranged in a triangular lattice. For monovalent anions X one electron is transferred from each dimer (ET)$_2$ to each anion formula unit. In effect, the dimer layers possess one hole per dimer and their highest occupied molecular orbitals (HOMO) give rise to a half-filled conduction band. Hence, band structure calculations[3,4] predict the dimer layers to be metallic. However, the experimentally observed ground state depends on the choice of the anion: even for the example of the isostructural compounds κ-(ET)$_2$Cu[N(CN)$_2$]Cl (in short κ-Cl) and κ-(ET)$_2$Cu[N(CN)$_2$]Br (κ-Br), the ground state can be as different as a Mott insulator for κ-Cl and a Fermi liquid for κ-Br at low temperatures and ambient pressure.[5] In fact, κ-Cl can be driven through the insulator-to-metal transition (MIT) by the gradual substitution of Cl for isovalent Br which changes the volume of the system and thereby decreases the ratio U/W of the Hubbard U to the band width W. Being close to the MIT, κ-Br is a 'good' (coherent) metal with a Drude peak only below a coherence temperature $T^* \approx 50$ K. At higher temperatures κ-Cl is a semiconductor with a gap of $E_g = 800$ K[7] while κ-Br shows 'bad metal' behavior with strong scattering preventing coherent transport and suppressing the Drude peak. Theoretically, this crossover from a Fermi liquid at low T to the 'bad' metal state at higher temperatures in κ-Br is obtained from dynamical mean field theory (DMFT) calculations where gradual destruction of coherent quasiparticles occurs with increasing temperature,[6] albeit at higher T^* than observed experimentally.

The fact that small chemical modifications lead to qualitative changes in behavior together with the importance of electronic correlations in these materials make it clear that a realistic description requires both (i) details of the band structure as well as (ii) a proper treatment of strong correlations. However, many-body studies of the κ-(ET)$_2X$ salts have so far been limited to minimal model calculations[6,8,9] of the Hubbard or extended Hubbard Hamiltonian on an anisotropic triangular lattice.[10] In this work, we go beyond model calculations and present a combination of ab-initio density functional theory calculations in the full potential linearized augmented plane wave (FLAPW) framework[11] combined with DMFT[12] (LDA+DMFT). With this approach, the above requirements for a realistic description of these systems are fulfilled to a large extent. To our knowledge, this is the first LDA+DMFT calculation on an organic molecular crystal. Specifically, we focus on the spectral and optical properties of κ-Cl at room temperature. While the kinetic part of the Hamiltonian is described with full DFT precision, we use a few values of the Hubbard interaction strength U in order to illuminate the effects of different U/W ratios. We will show that, whereas it is well known that the DMFT method does not yield a perfect description of the underlying Hubbard Hamiltonian on a triangular lattice in two dimensions, this approach provides insight into the contributions to the optical conductivity at an unprecedented level. Our calculations demonstrate that interdimer and intradimer transitions are responsible for two principal features observed in optical conductivity measurements at low temperatures and identify the interdimer feature to be related to correlations. These results corroborate previous conjectures based on phenomenological and minimal model assumptions.[13,14]

In order to perform LDA+DMFT calculations on molecular crystals we have to construct localized Wannier functions for molecular orbitals as required by DMFT.

The construction method based on projecting Bloch states onto pure atomic orbitals with subsequent orthonormalization[12,15,16] is fast and stable. In its standard form, though, the projection method is, by definition, not designed for molecular orbitals. In this work, we propose a scheme to construct molecular Wannier functions using atomic orbitals as a starting point. The key element of this scheme is the diagonalization of the occupation matrix written in the basis of atomic orbitals within the subspace of correlated bands.[17] The real space representation of the resulting dimer HOMO Wannier function of κ-Cl (based on the crystal structure reported in Ref. 18 with space group $Pnma$) is shown in Fig. 1.

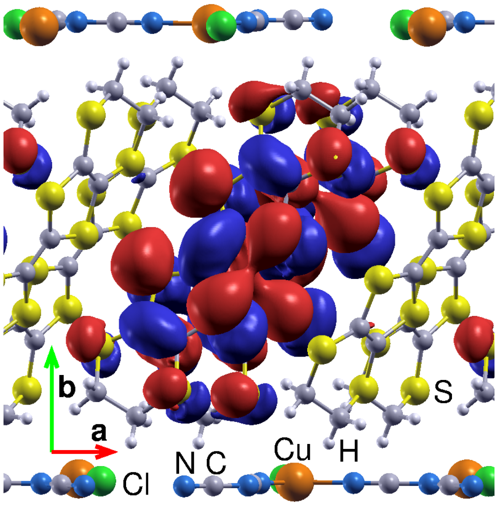

FIG. 1. (Color online) Structure of κ-(ET)$_2$Cu[N(CN)$_2$]Cl seen along the c axis with a Wannier function corresponding to the bands crossing the Fermi level.

For solving the impurity problem we employed the hybridization expansion continuous-time quantum Monte Carlo method[19] as implemented in the ALPS code[20,21] where we used 2×10^7 Monte Carlo sweeps throughout our calculations at an inverse temperature $\beta = 40$ eV^{-1}, corresponding to room temperature. Note that in the crystallographic unit cell, there is a manifold of four bands around E_F as the crystallographic unit cell contains two organic layers with a total of four dimers due to the presence of the anion. The dimers are equivalent, though, so that only one dimer HOMO has to be considered in our single-site DMFT; the other three orbitals are related by symmetry. Since the quantum Monte Carlo algorithm operates on the imaginary frequency axis, the calculation of dynamical quantities like spectral functions and optical conductivity requires analytic continuation to the real axis. We performed stochastic analytic continuation[22] on the self energy for obtaining the spectral functions and directly on the optical conductivity $\sigma(i\nu)$ for the calculation of optical properties.[23] Concerning appropriate interaction parameters for these systems, considerably distinct values for the Hubbard U have been reported. In this work we analyze the effect of the values $U = 0.5/0.6/0.7/0.84$ eV. This range is guided by two estimates: $U = 0.85$ eV obtained for a similar but arguably more strongly correlated compound κ-(ET)$_2$Cu$_2$(CN)$_3$ from constrained random phase approximation[4], and $U \approx 0.27$ eV extracted from optical conductivity measurements[13] and model considerations.[9]

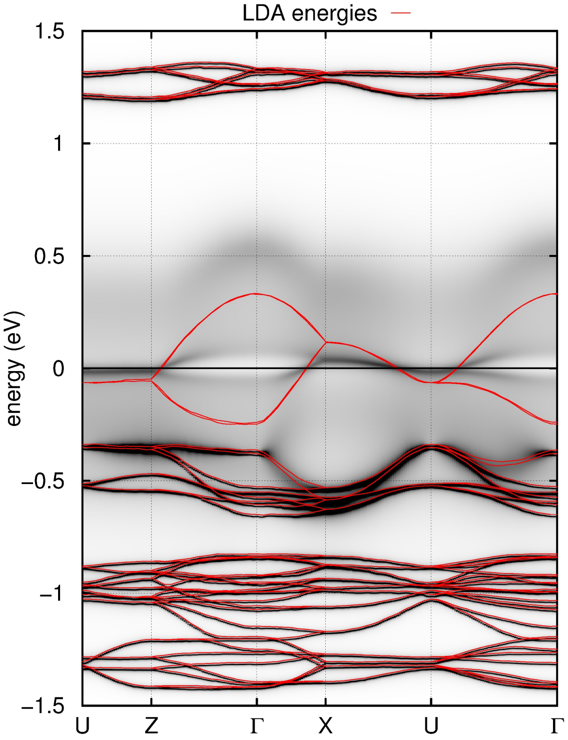

FIG. 2. (Color online) Momentum-resolved spectral function for $U = 0.6$ eV.

In Fig. 2 we show the calculated band structure of κ-Cl in form of the momentum-resolved spectral function for $U = 0.6$ eV along with the LDA band energies. The bands at the Fermi energy $E_F = 0$ originate from the interdimer hopping, in particular hopping between dimers on the same layer; the interlayer hopping is very small, so that the four bands are composed of two almost degenerate pairs of bands. The correlation in band space acts almost exclusively on these bands, splitting them into renormalized excitations of (mass-enhanced) quasiparticles and a spectral weight transfer to an upper and lower Hubbard band which manifests itself as blurry background. On the other side, the charge transfer between the ET molecules within a dimer (intradimer) induces the splitting between the bands right below the correlated manifold and the correlated bands. For uncorrelated states, the excitations basically lie on top of the respective LDA energies which validates the accuracy of our analytic continuation.

The development of the Hubbard bands with U is visible from the momentum-integrated spectral functions in Fig. 3. At E_F, the spectral functions are suppressed compared to LDA and Hubbard bands are formed for all values of U, getting more pronounced as U is increased; the maxima of the Hubbard peaks are located at $\omega \approx \pm U/2$, as expected. However, a quasiparticle peak at E_F remains present up to $U = 0.7$ eV; the largest value of U shown, $U = 0.84$ eV, is just on the verge of opening a gap at E_F. It is known, however, that the critical value of U for the MIT, U_c, is significantly overestimated by DMFT in low dimensions: for the triangular latice in two dimensions as in our case, DMFT yields $U_c \approx 15|t|$[9] whereas extrapolated cluster approximations[24] yield $U_c \approx 7|t|$.

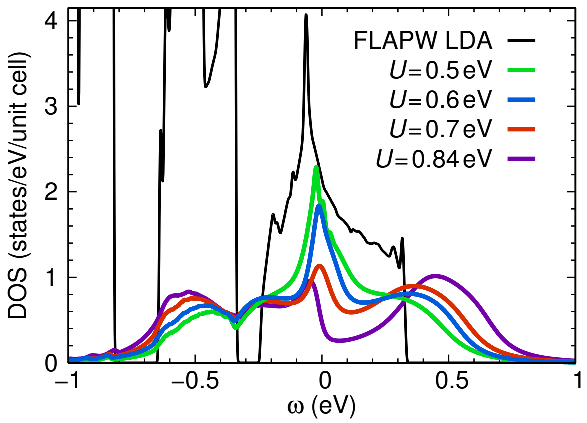

FIG. 3. (Color online) LDA density of states and the LDA+DMFT spectral functions for different values of U.

Next, we investigate the optical properties of κ-Cl where, like in previous works,[13,14] we concentrate on the polarization $E \parallel c$, *i. e.*, along the linear chains in the triangular lattice. The authors of Ref. 13 performed a comprehensive study on the evolution of the optical conductivity spectra from infrared reflection measurements on κ-(ET)$_2$Cu[N(CN)$_2$]Cl$_{1-x}$Br$_x$ tuned through the MIT by increasing the Br concentration x. At room temperature, they observed a broad midinfrared absorption peak between 1600 cm^{-1} and 4200 cm^{-1}, in agreement with previous optical studies on κ-Cl and κ-Br (see Ref. 13 and references therein). At low temperature, a Drude peak evolves for the compounds with high Br concentration which marks the onset of metallicity at $x \approx 0.7$ whereas no Drude peak is visible for lower Br content indicating an insulating state without coherent quasiparticles.

Importantly, at low temperatures the broad midinfrared peak splits into two peaks in the pure Cl and low Br concentration compounds, fitted by two Lorentzians at $\approx$2200 cm^{-1} and 3200 cm^{-1}; for high Br content this splitting is very weak. From this doping dependence, it was concluded[13] that the first peak is a correlation-induced feature due to electron transitions between the lower and upper Hubbard bands, while the second 'dimer peak' was assigned to the intradimer charge transfer. For the metallic Br rich compounds, the spectral weight transfer from the Drude peak to this Hubbard peak is small and the Hubbard peak is suppressed or less pronounced. Since the Hubbard peak is expected to appear at $\omega \approx U$, this would determine the effective U as $U \approx 2200$ cm^{-1} $= 0.27$ eV.

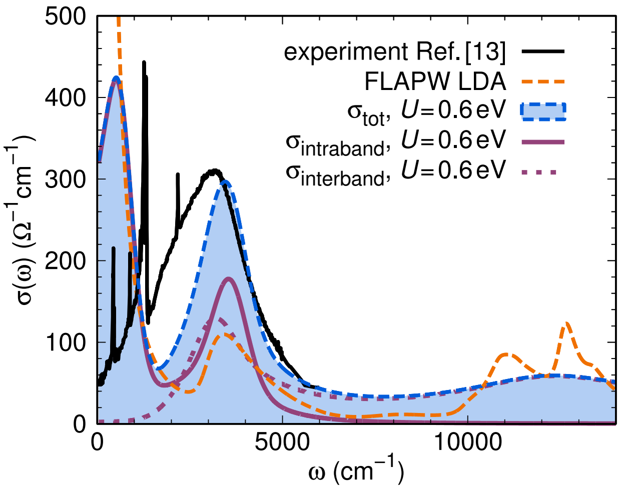

FIG. 4. (Color online) Calculated LDA+DMFT optical conductivity for $U = 0.6$ eV together with the LDA result and the experimental curve at $T = 300$ K.

Our method allows us to test this interpretation; as the energy window of our LDA+DMFT calculation contains both the correlated manifold at the Fermi energy as well as uncorrelated bands away from E_F, all transitions can be inspected on equal footing. As mentioned above, the symmetry of the organic layers is higher than the symmetry of the crystal, therefore the four bands around E_F can be considered to originate from one band which is folded due to the unit cell that is twice as large as required by ET layer symmetry. These bands thus create the *intra*band contribution to the optical conductivity discussed in the following; physically they correspond to the *inter*dimer hopping. All other transitions are termed *inter*band transitions; among others, these contain transitions related to the *intra*dimer charge transfer.

The LDA+DMFT calculated optical conductivity for $U = 0.6$ eV together with the experimentally measured spectrum of κ-Cl at $T = 300$ K is shown in Fig. 4. Overall, the calculated total optical conductivity σ_{tot} features one dominant peak at approximately 3450 cm^{-1}, *i. e.*, close to the experimental peak position (we do not consider vibronic modes),[13] and a second much higher-frequency peak between 8000 cm^{-1} and 17000 cm^{-1}. The peak at higher frequencies originates from interband transitions between uncorrelated states and hence corresponds in frequency with LDA (also shown in the figure); the analytic continuation smears out the fine structure of this peak. The position of the low-frequency peak of σ_{tot} is roughly centered at the same position as the LDA results, but it is strongly enhanced in spectral weight, in accordance with experiment. While our calculations are at room temperature, they already capture the effects of correlation observed more pronounced in measurements at low T. Decomposed into intra- and interband contributions, we find that $\sigma_{\text{interband}}$ roughly coincides with the LDA results in position and spectral weight. In addition, we find an intraband absorption at $\omega \approx 3550\text{cm}^{-1} \approx 0.75\,U$ which we identify as intraband Hubbard transitions. While one expects a peak at $\omega \approx U$ from transitions between the Hubbard bands, a $U/2$ peak mixes in since a quasiparticle peak is still present in our calculations (for the chosen $U = 0.6$ eV) and allows for transitions between the quasiparticle peak and the Hubbard bands. Accordingly, our data show a remnant of the Drude peak not observed experimentally for the pure Cl compound. The previously mentioned limitations of DMFT here force us in our choice of U values to compromise between the correct semiconducting phase (favored by a large U) and the correct Hubbard peak position (favored by a moderate U).

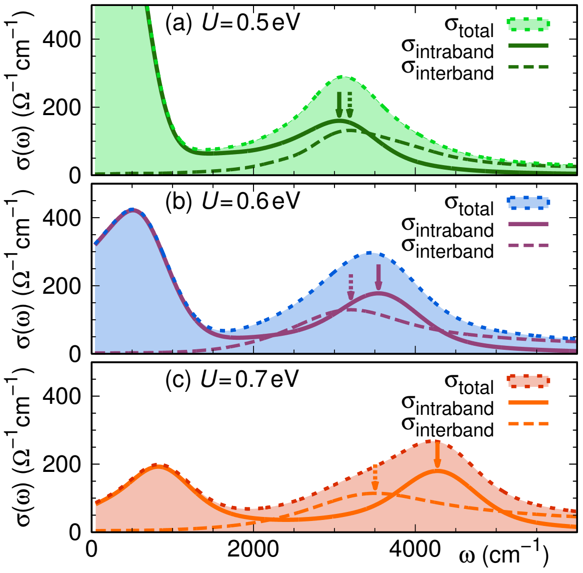

FIG. 5. (Color online) Optical conductivities for different values of U. The peak positions of the intraband (interband) contribution are: $\omega \approx 3000\,(3200)$ cm^{-1} for $U = 0.5$ eV, $\omega \approx 3550\,(3200)$ cm^{-1} for $U = 0.6$ eV, and $\omega \approx 4250\,(3500)$ cm^{-1} for $U = 0.7$ eV. The arrows show the respective peak positions.

As for the nature of the absorption peaks, Fig. 5 shows their evolution with U. The intraband contribution to the conductivity moves in frequency proportional to U, with the peak position consistently corresponding to $\approx 0.75\,U$ while the interband absorption is largely insensitive to U. This analysis demonstrates the correlated nature of $\sigma_{\text{intraband}}$ and uncorrelated nature of $\sigma_{\text{interband}}$. In all cases, the two peaks are too close to each other to be individually resolved from the total optical conductivity alone. Furthermore, Fig. 5 shows how the Drude peak develops for decreasing U values; Fig. 5 (a) with $U = 0.5$ eV is actually similar to the case of κ-Br as analyzed in Fig. 8 of Ref. 13.

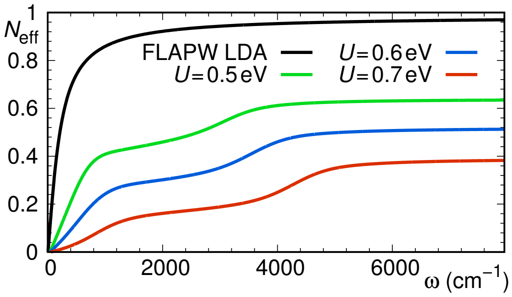

FIG. 6. (Color online) Distribution of the intraband spectral weight in terms of the effective number of charge carriers.

Quantitatively, the suppression of the Drude peak as a function of U and the redistribution of the intraband spectral weight is presented in Fig. 6 where we follow Ref. 9 and plot the integrated spectral weight $\int_0^{\omega} \sigma_{\text{intraband}}(\omega')d\omega'$ representing the effective number of charge carriers N_{eff}. In this representation, the number of charge carriers in LDA by definition equals the number of conduction electrons, *i. e.* one, and all the weight is concentrated in the (infinitesimally narrow) coherent Drude peak which is only broadened by temperature. Upon inclusion of correlations, the kinetic energy of the electrons is diminished, which corresponds to mass enhancement (in Fermi liquid theory) or a reduction of the number of effective charge carriers as we observe.

Summarizing the analysis of the optical conductivity calculations, we find agreement with the principal assessment of Ref. 13, namely that the two finite-frequency peaks in the experimental optical conductivity of κ-Cl at low temperatures originate, respectively, from correlation-induced intraband (interdimer) contributions ('Hubbard peak'), scaling with U, and interband (intradimer) transitions which are unaffected by correlations ('dimer peak'). The fact that DMFT overestimates the critical U of the triangular lattice in two dimensions forces us to describe κ-Cl with a somewhat high interaction strength of U=0.6 eV, suggesting that future studies combining LDA with many-body techniques beyond DMFT like cluster extensions of DMFT[25] may further improve the quantitative agreement with experimental measurements. This is beyond the scope of the present study.

In conclusion, we presented the first LDA+DMFT study on the spectral and optical properties of the organic CT salt κ-(ET)$_2$Cu[N(CN)$_2$]Cl. Our results provide an *ab initio*-based theoretical evidence for the double-natured origin of the infrared peak in the optical conductivity of κ-(ET)$_2$Cu[N(CN)$_2$]Cl. We could identify intraband transitions within the correlated manifold and interband transitions due to charge-transfer within an ET dimer. The proposed projection method for constructing non-atom-centered Wannier functions in the FLAPW framework is computationally efficient and can be applied to a great variety of correlated organic as well as inorganic systems with (quasi-)molecular orbitals.

We gratefully acknowledge financial support from the Deutsche Forschungsgemeinschaft through TR49 and FOR1346 and the allotment of computer time by CSC-Frankfurt and LOEWE-CSC. H.O.J. thanks the Helmholtz association for support through HA216/EMMI.

---

* ferber@itp.uni-frankfurt.de

[1] K. Kanoda and R. Kato, Annu. Rev. Condens. Matter Phys. **2**, 167 (2011).

[2] B. J. Powell and R. H. McKenzie, Rep. Prog. Phys. **74**, 056501 (2011).

[3] H. C. Kandpal, I. Opahle, Y.-Z. Zhang, H. O. Jeschke, and R. Valentí, Phys. Rev. Lett. **103**, 067004 (2009).

[4] K. Nakamura, Y. Yoshimoto, T. Kosugi, R. Arita, and M. Imada, J. Phys. Soc. Jpn. **78**, 083710 (2009).

[5] Below 35 K, κ-(ET)$_2$Cu[N(CN)$_2$]Cl develops a weak magnetic order[26,27] whereas κ-(ET)$_2$Cu[N(CN)$_2$]Br enters a superconducting state at $T_c = 12$ K.[28] We are not considering these very low temperature phases here.

[6] J. Merino and R. H. McKenzie, Phys. Rev. B **61**, 7996 (2000).

[7] S. Yasin, M. Dumm, B. Salameh, P. Batail, C. Mézière, and M. Dressel, Eur. Phys. J. B **79**, 383 (2011).

[8] O. Parcollet, G. Biroli, and G. Kotliar, Phys. Rev. Lett. **92**, 226402 (2004).

[9] J. Merino, M. Dumm, N. Drichko, M. Dressel, and R. H. McKenzie, Phys. Rev. Lett. **100**, 086404 (2008).

[10] B. J. Powell and R. H. McKenzie, J. Phys.: Condens. Matter **18**, R827 (2006).

[11] P. Blaha, K. Schwarz, G. K. H. Madsen, D. Kvasnicka, and J. Luitz, *WIEN2k, An Augmented Plane Wave + Local Orbitals Program for Calculating Crystal Properties* (Techn. Universität Wien, Austria, 2001).

[12] M. Aichhorn, L. Pourovskii, V. Vildosola, M. Ferrero, O. Parcollet, T. Miyake, A. Georges, and S. Biermann, Phys. Rev. B **80**, 085101 (2009).

[13] D. Faltermeier, J. Barz, M. Dumm, M. Dressel, N. Drichko, B. Petrov, V. Semkin, R. Vlasova, C. Meźière, and P. Batail, Phys. Rev. B **76**, 165113 (2007).

[14] M. Dumm, D. Faltermeier, N. Drichko, M. Dressel, C. Mézière, and P. Batail, Phys. Rev. B **79**, 195106 (2009).

[15] W. Ku, H. Rosner, W. E. Pickett, and R. T. Scalettar, Phys. Rev. Lett. **89**, 167204 (2002).

[16] V. I. Anisimov, D. E. Kondakov, A. V. Kozhevnikov, I. A. Nekrasov, Z. V. Pchelkina, J. W. Allen, S.-K. Mo, H.-D. Kim, P. Metcalf, S. Suga, A. Sekiyama, G. Keller, I. Leonov, X. Ren, and D. Vollhardt, Phys. Rev. B **71**, 125119 (2005).

[17] See the Supplementary Material for a detailed description of the method.

[18] J. M. Williams, A. M. Kini, H. H. Wang, K. D. Carlson, U. Geiser, L. K. Montgomery, G. J. Pyrka, D. M. Watkins, J. M. Kommers, S. J. Boryscuk, A. V. S. Crouch, W. K. Kowk, J. E. Schirber, D. L. Overmyer, D. Jung, M.-H. Whangbo, Inorg. Chem. **29**, 3272 (1990).

[19] P. Werner, A. Comanac, L. de' Medici, M. Troyer, and A. J. Millis, Phys. Rev. Lett. **97**, 076405 (2006).

[20] B. Bauer, L. D. Carr, H. G. Evertz, A. Feiguin, J. Freire, S. Fuchs, L. Gamper, J. Gukelberger, E. Gull, S. Guertler, A. Hehn, R. Igarashi, S. V. Isakov, D. Koop, P. N. Ma, P. Mates, H. Matsuo, O. Parcollet, G. Pawłowski, J. D. Picon, L. Pollet, E. Santos, V. W. Scarola, U. Schollwöck, C. Silva, B. Surer, S. Todo, S. Trebst, M. Troyer, M. L. Wall, P. Werner, and S. Wessel, J. Stat. Mech. , P05001 (2011).

[21] E. Gull, P. Werner, S. Fuchs, B. Surer, T. Pruschke, and M. Troyer, Comp. Phys. Commun. **182**, 1078 (2011).

[22] K. S. D. Beach, arXiv:cond-mat/0403055 (unpublished).

[23] While we could have used the analytically continued self energy also for the calculation of $\sigma(\omega)$ on the real axis, we chose to calculate $\sigma(i\nu)$ on the imaginary frequency axis and proceed with a subsequent analytic continuation for performance reasons: the summation over all elements of the four-index conductivity tensor along with the frequency convolution involved in the calculation of σ scales as $N_b^4 \cdot N_f^2$ where N_b is the number of bands ($N_b = 44$) and N_f the number of frequencies. While in imaginary frequencies N_f can be of the order of 100 at the temperature we considered, an accurate determination on the real frequency axis would require $N_f \approx 1000$. Due to the large number of bands involved in our calculations, this would make the direct real-frequency calculation of σ rather expensive.

[24] P. Sahebsara and D. Sénéchal, Phys. Rev. Lett. **100**, 136402 (2008).

[25] H. Lee, K. Foyevtsova, J. Ferber, M. Aichhorn, H. O. Jeschke, and R. Valentí, Phys. Rev. B **85**, 165103 (2012).

[26] K. Miyagawa, A. Kawamoto, Y. Nakazawa, and K. Kanoda, Phys. Rev. Lett. **75**, 1174 (1995).

[27] K. Kanoda, Physica C **282-287**, 299 (1997).

[28] A. M. Kini, U. Geiser, H. H. Wang, K. D. Carlson, J. M. Williams, W. K. Kwok, K. G. Vandervoort, J. E. Thompson, and D. L. Stupka, Inorg. Chem. **29**, 2555 (1990).